

Optical Navigation for Hayabusa2 Approaching Phase

Yuki TAKAO^{1)†}, Yuya MIMASU²⁾, and Yuichi TSUDA²⁾

¹⁾Department of Aeronautics and Astronautics, The University of Tokyo, Tokyo 113-8656, Japan

²⁾Institute of Space and Astronautical Science, Japan Aerospace Exploration Agency, Sagamihara, Kanagawa 252-5210, Japan

This paper presents the results of optical navigation performed by the asteroid explorer Hayabusa2 in approaching phase using the images of the asteroid Ryugu. The determination accuracy of the relative distance between the spacecraft and asteroid is crucial in navigation of approaching phase. This relative distance can be estimated from the size of the asteroid in the images, but this calculation requires the actual radius of the asteroid with high accuracy. We have estimated the relative distance from the change rate of the asteroid area in the images, without relying on such prior information as asteroid radius. Additionally, the actual radius of the asteroid has also been estimated using the relative distance estimated.

1. Introduction

The asteroid explorer Hayabusa2, launched by the Japan Aerospace Exploration Agency in 2014, has arrived at the asteroid Ryugu on June 29, 2018. The probe had been driven mainly by ion engines in combination with Earth gravity assist. At the very last phase of rendezvous, the probe turned off the ion engines and used chemical propulsion instead to perform trajectory correction maneuvers (TCMs); the orbit determination errors of both the asteroid and probe were corrected based on the navigation results relative to the asteroid.

The navigation methods used in this approaching phase use optical or radiometric information. Actually, the Hayabusa2 mission used hybrid navigation using both optical and radiometric observations. This navigation method is based on the concept of triangulation: the relative position between the spacecraft and asteroid is reconstructed from the direction in which the asteroid is observed. However, the estimation results vary in this case because the precise value of the base length is unknown. In particular, the variance is large in the distance direction. Hayabusa2 had determined the relative position taking into account the past estimation results so that all data match the trajectory.

The above-stated navigation method considers the asteroid as a point mass. However, the images of the asteroid become more than a single pixel as the spacecraft gets close to the asteroid; the information about the asteroid size becomes available, which in turn gives us the relative distance.

This paper presents the optical navigation method that is used to estimate the distance relative to the asteroid. The asteroid size in images is defined quantitatively so that it can be related to the relative distance. The actual navigation results in the approaching phase of the Hayabusa2 mission are shown, comparing them with the triangulation-based methods. In addition, the estimation results of the asteroid size in the real space (NOT in the images) are provided based on the relative distance estimation.

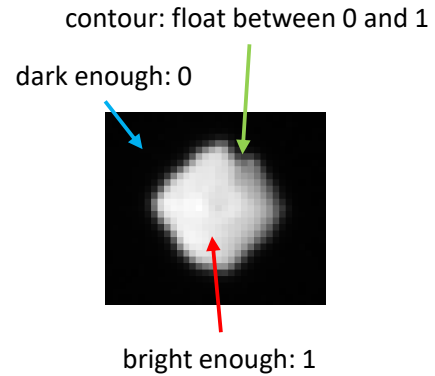


Fig. 1: Filtering of pixel values.

2. Navigation Method

2.1. Pixel Area

The asteroid size in images is defined by introducing the idea of pixel area. Pixel area is the number of pixels occupied the image of the asteroid. It can be calculated using binarization because the asteroid image is bright and the background is dark; therefore, the pixel area is the number of pixels that have HIGH values after binarization.

It is clear from the definition above that the value of pixel area is integer. This may worsen the estimation results because the value increases discontinuously as the spacecraft approaches the asteroid; this effect is remarkable when the relative distance is large because of the low resolution of the asteroid image.

To deal with this problem, the pixel area is extended to float value by smoothing the contour of the asteroid. Letting l denote a luminance of the image, the contour is smoothed using the following filter:

$$f(l) = \begin{cases} 1 & \text{if } l > l_{\text{high}} \\ 0 & \text{if } l < l_{\text{low}} \\ \frac{l-l_{\text{low}}}{l_{\text{high}}-l_{\text{low}}} & \text{else} \end{cases} \quad (1)$$

where l_{high} and l_{low} are the higher and lower threshold of filtering. The pixels corresponding to the contour has luminance values between 0 and 1 by applying this filter. Figures 1 and 2 summarize the idea of filtering. The pixel area can

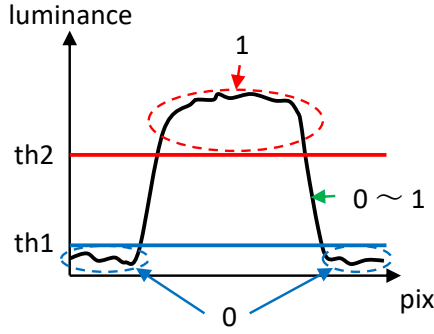


Fig. 2.: Thresholding for pixel area calculation.

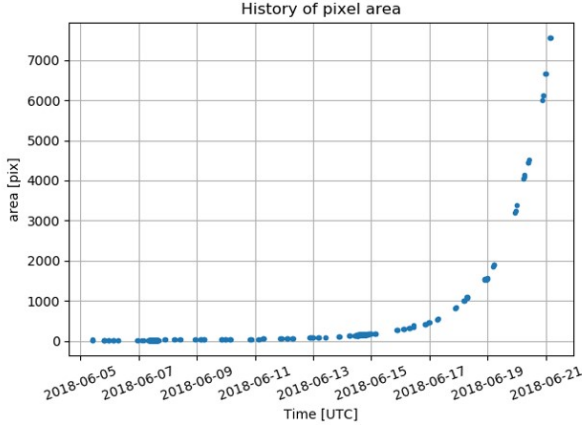


Fig. 3.: History of pixel area during the Hayabusa2 approaching phase.

be calculated with float-level accuracy by summing up all the luminance values of the filtered image. Figure 3 shows the history of pixel area during the approaching phase of the Hayabusa2 mission.

2.2. Relative Distance Estimation

Assuming that the asteroid is a sphere with the radius of R , it is projected on the camera screen as a circle with the radius of:

$$R_{\text{img}} = \frac{fR}{pz} \quad (2)$$

where f is focal length, p is the size of a pixel, and z is the relative distance between the spacecraft and asteroid. Hence, the pixel area and relative distance are related as follows.

$$\begin{aligned} A &= \pi R_{\text{img}}^2 \\ &= \pi \left(\frac{fR}{p} \right)^2 z^{-2} \end{aligned} \quad (3)$$

Although the relative distance z can be obtained by solving Eq. (3), there are actually various error factors that:

1. the asteroid is not a sphere actually
2. the estimation of the equivalent radius R that is available before arrival is inaccurate
3. the calculated pixel area includes observation error

Therefore, the solution of Eq. (3) is not sufficient as the estimation of the relative distance.

In this paper, we provide an alternative method that estimates the relative distance with higher accuracy. The ratio of the pixel area and relative distance is considered to remove

the uncertainty of the asteroid radius. Given that two observations at different time, t_i and t_j , are obtained, the following equation is derived using Eq. (3).

$$\frac{z(t_j)}{z(t_i)} = \sqrt{\frac{A(t_i)}{A(t_j)}} := \beta_{ij} \quad (4)$$

Equation (4) can be rewritten as follows.

$$z(t_i) = \frac{\Delta z_{ij}}{\beta_{ij} - 1} \quad (5)$$

where

$$\Delta z_{ij} = z(t_j) - z(t_i) \quad (6)$$

Equation (5) suggests that the distance relative to the asteroid can be obtained once the relative displacement in the distance direction, Δz_{ij} is given. This relative displacement can be calculated with high accuracy by integrating the history of velocity; their relative velocity is known with a few mm/s accuracy owing to Doppler measurement. Finally, the relative distance at time t_i is given by:

$$z(t_i) = \frac{\int_{t_i}^{t_j} v_z(t) dt}{\beta_{ij} - 1} \quad (7)$$

Equation (7) shows that a time different from the target time must be determined. In the followings, a method to determine the comparison time t_j against the target time t_i based on the idea of error analysis.

An observation error is defined against the observable A ; we assume that the observation error ΔR_{img} can be defined against equivalent radius R_{img} . Then, the parameter β_{ij} , defined in Eq. (4), under observation error can be expressed as follows.

$$\begin{aligned} \beta_{ij} + \Delta \beta_{ij} &= \sqrt{\frac{A(t_i) \pm \Delta A(t_i)}{A(t_j) \mp \Delta A(t_j)}} \\ &= \sqrt{\frac{\pi \{R_{\text{img}}(t_i) \pm \Delta R_{\text{img}}\}^2}{\pi \{R_{\text{img}}(t_j) \mp \Delta R\}^2}} \\ &= \frac{\sqrt{A(t_i)/\pi} \pm \Delta R_{\text{img}}}{\sqrt{A(t_j)/\pi} \mp \Delta R} \end{aligned} \quad (8)$$

The maximum and minimum values of β_{ij} are:

$$\begin{aligned} \beta_{ij}^{\text{max}} &= \frac{\sqrt{A(t_i)/\pi} + \Delta R}{\sqrt{A(t_j)/\pi} - \Delta R_{\text{img}}} \\ \beta_{ij}^{\text{min}} &= \frac{\sqrt{A(t_i)/\pi} - \Delta R}{\sqrt{A(t_j)/\pi} + \Delta R_{\text{img}}} \end{aligned} \quad (9)$$

Thus, the estimation error of $z(t_i)$ can be given as follows.

$$\frac{\int_{t_i}^{t_j} v_z(t) dt}{\beta_{ij}^{\text{max}} - 1} \leq z(t_i) \leq \frac{\int_{t_i}^{t_j} v_z(t) dt}{\beta_{ij}^{\text{min}} - 1} \quad (10)$$

The following trade-offs can be considered against the selection of t_j :

- $|t_j - t_i|$ is large:
 - estimation converges because $\beta_{ij} - 1$ is large enough
 - observation error is large

Table 1.: Comparison of the methods

t_i (UTC)	pixel-area-based method			triangulation-based methods			
	$z(t_i)$ [km]	Δz^+ [km]	Δz^- [km]	No.1 [km]	No.2 [km]	No.3 [km]	No.4 [km]
2018/06/17 21:00:00	267.539	46.320	33.073	244.795	267.840	264.435	239.518
2018/06/19 21:00:00	146.758	11.061	9.409	138.214	136.218	111.066	126.535

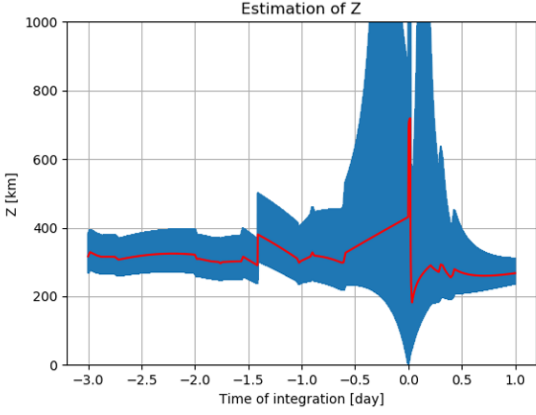


Fig. 4.: Estimation of z at 2018/06/17 21:00:00 (UTC).

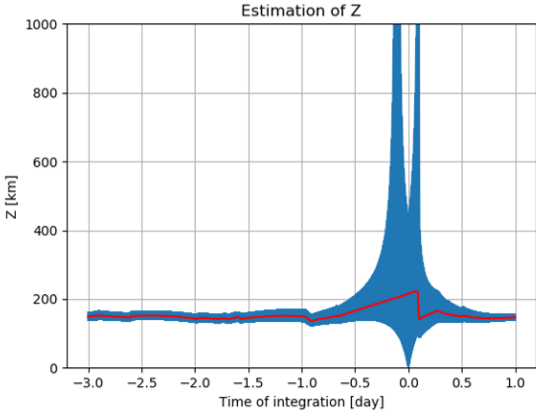


Fig. 5.: Estimation of z at 2018/06/19 21:00:00 (UTC).

- $|t_j - t_i|$ is small:
 - estimation diverges because $\beta_{ij} - 1$ is close to zero
 - observation error is small

Hence, it can be considered that there is the optimal time t_j that minimizes the estimation error; the optimal value of t_j is given as the time that minimizes the error bar of $z(t_i)$.

3. Navigation Results in Hayabusa2 Mission

3.1. Estimation at a single time

Some examples of distance estimation are shown. The observation error is given as $\Delta R_{\text{img}} = 1$ pix. Figure 4 shows the plots of $z(t_i)$ with the target time of $t_i = 2018/06/17$ 21:00:00 (UTC) against different comparison time t_j . The horizontal axis denote $t_j - t_i$ [day]. The red line is the estimation of $z(t_i)$ calculated from Eq. (7), and the blue lines are the error bar of $z(t_i)$ derived from Eq. (10). As can be seen from the figure, the estimation error diverges when $t_j - t_i \approx 0$ and is small when $t_j - t_i$ is sufficiently large. The most-likely estimation

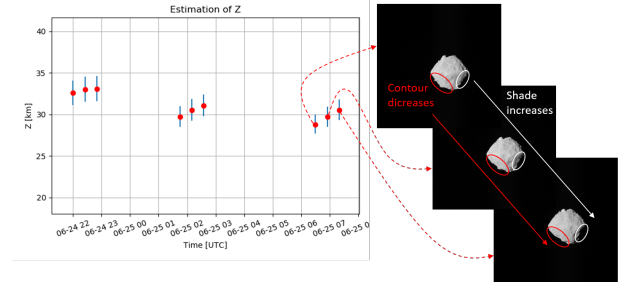


Fig. 6.: Estimation history and the effect of rotation.

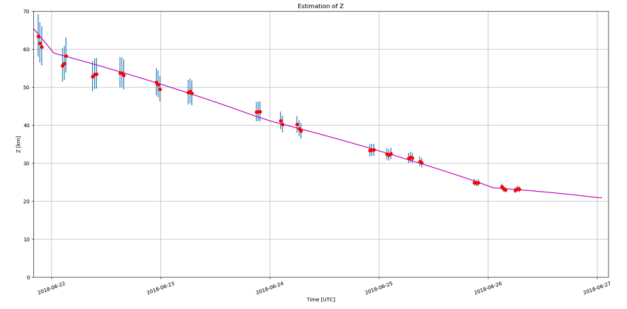


Fig. 7.: Fitting result.

of $z(t_i)$ is as follows.

$$\left. \begin{aligned} z(t_i) &= 267.539 \text{ [km]} \\ \Delta z^+(t_i) &= 46.320 \text{ [km]} \\ \Delta z^-(t_i) &= 33.073 \text{ [km]} \end{aligned} \right\} \text{ at } t_i = 2018/06/17 \text{ 21:00:00 (UTC)}$$

Figure 5 shows another example at $t_i = 2018/06/19$ 21:00:00 (UTC). It confirms the similar trend as in Fig. 4. The final estimation of $z(t_i)$ is:

$$\left. \begin{aligned} z(t_i) &= 146.758 \text{ [km]} \\ \Delta z^+(t_i) &= 11.061 \text{ [km]} \\ \Delta z^-(t_i) &= 9.409 \text{ [km]} \end{aligned} \right\} \text{ at } t_i = 2018/06/19 \text{ 21:00:00 (UTC)}$$

These results show that the estimation error gets smaller as the spacecraft approaches the asteroid. The reason for this is because the pixel area observed in the images gets large compared to observation error.

Table 1 compares the pixel-area-based estimation results to the triangulation-based ones. There are four triangulation-based results that use different methods and data. They confirm that the results of the pixel-area-based method match those of the triangulation-based methods.

3.2. Continuous Estimation

The analysis above has shown that the distance relative to the asteroid can be estimated using the information about the asteroid size. When the spacecraft gets closer to the asteroid, however, the pixel-area-based method may return inappropriate result: Fig. 6 shows that the relative distance gets larger as time proceeds, which is impossible because the spacecraft is actually getting closer to the asteroid. The reason for this error is because of the rotation of the asteroid. As shown in Fig.

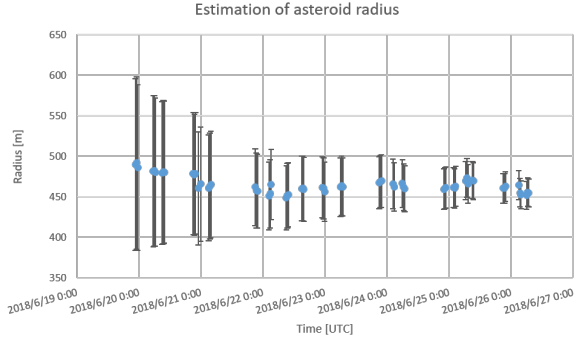


Fig. 8.: Estimation of the mean asteroid radius.

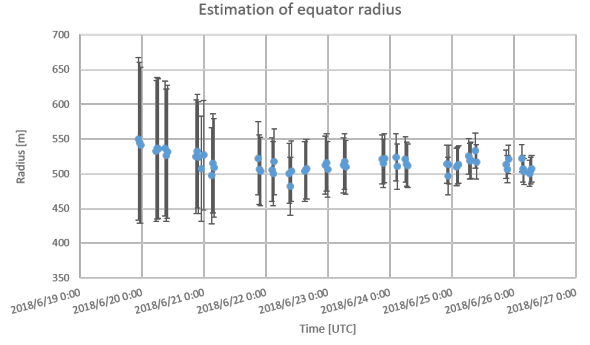


Fig. 9.: Estimation of the maximum asteroid radius.

6, pixel area may decrease as the asteroid rotates, even if the relative distance is getting small. This phenomenon happens when the resolution of the asteroid image is high because of close distance.

To deal with this, the trajectory of the spacecraft is taken into account. In concrete, the integration of the spacecraft velocity gives the time history of the relative distance. The constant of integration is determined by fitting the trajectory to the discrete estimation results. The weighted least squares method is used here; the estimation error of $z(t_i)$ shown in Eq. (10) is regarded as 1σ range.

Figure 7 shows the fitting result. The most-likely time history of the relative distance is obtained by combining the pixel-area-based estimation and the integration of velocity. The figure also confirms that the fitting result is almost within the 1σ error range of each data, which means that every single estimation is valid. This suggests that the pixel-area-based estimation works even if the relative distance is large.

4. Asteroid Size Estimation

Once the distance relative to the asteroid is given, the size of the asteroid in the real space can be estimated. The asteroid radius R can be solved, from Eq. (3), as follows.

$$R = \frac{p}{f} \sqrt{\frac{A(t_i)}{\pi}} z(t_i) \quad (11)$$

Given that the observation error is ΔR_{img} and estimation error of $z(t_i)$ is Δz , the estimation error of R is derived as:

$$\Delta R = \frac{p}{f} \left(\sqrt{\frac{A(t_i)}{\pi}} \Delta z + z \Delta R_{\text{img}} \right) \quad (12)$$

Figure 8 shows the estimation result of the equivalent radius at different time. As can be seen, the estimation error of R gets small as time proceeds. This is because the estimation error of $z(t_i)$ also gets small. The weighted average of these data gives the expectation of R :

$$\hat{R}_{\text{mean}} = 461.21 \pm 14.24$$

Since the shape of Ryugu is similar to a diamond, it can be considered that the radius is maximum at the equator. The maximum radius can also be estimated by measuring the pixel length of diameter of the asteroid image. The pixel length D_{img} is defined as the number of pixels on the equator

Table 2.: Comparison of asteroid radius.

	mean radius [m]	maximum radius [m]
image-based	461.21 ± 14.24	512.08 ± 17.05
shape model	444.668	528.207

of the asteroid image. It is measured by counting the pixels that have HIGH values after binarization on the equator, in the same manner as measuring pixel area. The maximum radius at the equator is then derived as follows.

$$R_{\text{max}} = \frac{p}{f} \frac{D_{\text{img}}}{2} z(t_i) \quad (13)$$

The estimation error is:

$$\Delta R_{\text{max}} = \frac{p}{f} \left(z(t_i) \Delta R_{\text{img}} + \frac{D_{\text{img}}}{2} \Delta z \right) \quad (14)$$

Figure 9 shows the estimation results of the maximum radius. The estimation also converges similarly as the case of the mean radius. The expectation of the maximum radius is:

$$\hat{R}_{\text{max}} = 512.08 \pm 17.05$$

After the arrival at Ryugu, the Hayabusa2 project has constructed a 3D shape model of the asteroid based on precise observations.¹⁾ Now that the accurate shape and size of the asteroid are available, the accuracy of the size estimation which is based on the pixel-area method can be evaluated. Table 1 shows the mean and maximum radius estimated from the above-stated method, and the actual values calculated from the shape model. It turns out that the estimations obtained from the images in the approaching phase are close to the actual values that are revealed after precise observations.

5. Conclusion

An optical navigation method that was used in the Hayabusa2 mission to estimate the distance relative to the asteroid was presented. The estimation method is based on simple equations, but the results show that they give sufficiently accurate estimations. Even though the estimations are discrete, the continuous history of the relative distance can also be obtained using data fitting method.

In the actual operations in Hayabusa2, the results of the triangulation-based methods tended to split into two different values, depending on the data used. It is important to determine which value is more likely. The pixel-area-based method was able to suggest which solution to choose. It is

expected that the developed method can also be effective in the future asteroid exploration missions.

In addition, the size of the asteroid in the real space was estimated using the results of the relative distance estimation. Since the resolution of ground observation is not high enough, the accurate size of the asteroid is unknown until the probe reaches it. The developed method allows estimating the approximate size of the asteroid before arrival. This can be helpful not only to navigation but also to scientific obser-

ventions.

References

- 1) N. Hirata, N. Hirata, S. Tanaka, N. Nishikawa, T. Sugiyama, R. Gaskell, E. Palmer, R. Noguchi, Y. Shimaki, Matsumoto, *et al.*, "Initial results of shape modeling on the asteroid Ryugu from observations by Hayabusa2 for landing site selection," *Division for Planetary Sciences Meeting Abstracts*, Vol. 50, Knoxville, Tennessee, American Astronomical Society, Oct. 2018.